University of Tehran Press

Journal of the Earth and Space Physics

Homepage: https://jesphys.ut.ac.ir

Vol. 49, No. 4, Winter 2024, P. 93- 104

(Research Article)

Fuzzy Seismic Inversion: A Case Study on Channel Features in Johnson Formation of Browse Basin, Australia

Jahanjooy, S.[1] | Hashemi, H.[1] | Bagheri, M.[1]

1. Department of Earth Physics, Institute of Geophysics, University of Tehran, Tehran, Iran.

Corresponding Author E-mail: hashemy@ut.ac.ir

(Received: 18 Aug 2023, Revised: 4 Nov 2023, Accepted: 9 Jan 2024, Published online: 20 Feb 2024)

Abstract

Subsurface channels are stratigraphic features in seismic data that can act as reservoirs or conduits for hydrocarbons. However, detecting and characterizing these channels is challenging due to the limitations of seismic resolution and the complexity of the subsurface geology. Seismic inversion is a technique that can enhance the seismic data by transforming the seismic traces into quantitative estimates such as acoustic impedance (AI), which is a key reservoir rock property. AI inversion can help to identify and delineate the subsurface channels by providing more contrast and detail of the channel geometry, fill, and surrounding sediments. Seismic inversion is often challenged by the non-uniqueness, ambiguity and uncertainty of the inversion results due to noise and band-limited data. This paper uses a fuzzy model-based seismic inversion method that integrates prior information and fuzzy clustering constraints to produce more realistic and reliable AI models. This method assigns data points to multiple clusters with varying degrees of membership, which can capture the overlapping of AI values of different geological formations. The method is applied to the 3D Poseidon seismic data from the Browse Basin, offshore Western Australia, and the results are compared with those of conventional model-based inversion. Since there is no well-data in an interest channel zone, a qualitative evaluation with seismic attributes is performed. The subsurface structures are further interpreted by various seismic attributes. The comparison shows that the fuzzy model-based inversion method can improve the resolution, contrast and stability of the AI models and reveal more detail of the subsurface geology.

Keywords: Fuzzy seismic inversion, Acoustic impedance, Fuzzy clustering, Seismic attributes, RGB blending.

1. Introduction

Seismic data are the primary source of information for subsurface exploration and characterization. However, seismic data are band-limited and the traces can miss low and high frequency variations and features of the subsurface. Seismic inversion is a technique that aims to convert seismic traces into quantitative estimates of the reservoir rock properties, such as acoustic impedance, P and S-wave velocities, density, porosity, and fluid content (Bosch et al., 2010). Seismic inversion enhances the resolution and reliability of the seismic data and improves reservoir characterization and management (Rosa et al., 2020).

There are numerous pre-stack and post-stack seismic inversion methods. Pre-stack inversion utilizes the amplitude variation with offset (AVO) information to infer the elastic properties of the rocks, while post-stack inversion uses only the amplitude information to infer the acoustic impedance (Das & Mukerji, 2020). Recently, deep learning methods have been proposed to perform the seismic inversion directly from imaged seismic data, bypassing the conventional inversion steps and providing a fast and accurate alternative for litho-type classification (Pintea et al., 2021).

Seismic inversion models are non-unique and ambiguous. Having prior information about subsurface geology, such as well logs, rock physics models, or geostatistical models, can constrain seismic inversion results and increase the uniqueness of the results (Russell & Hampson, 1991). These methods iteratively update the initial model from the

Cite this article: Jahanjooy, S., Hashemi, H., & Bagheri, M. (2024). Fuzzy Seismic Inversion: A Case Study on Channel Features in Johnson Formation of Browse Basin, Australia. *Journal of the Earth and Space Physics*, 49(4), 93- 104. DOI: http//doi.org/10.22059/jesphys.2024.363747.1007551

E-mail: (1) saber.jahanjooy@ut.ac.ir | majidbagheri@ut.ac.ir

Publisher: University of Tehran Press.

DOI: http//doi.org/10.22059/jesphys.2024.363747.1007551

Print ISSN: 2538-371X

Online ISSN: 2538-3906

prior information until it matches the observed seismic data within a certain error tolerance (Das & Mukerji, 2020). This creates a higher resolution, better stability, and more realistic results (Pintea et al. 2021).

Constraining the inversion results into a predefined number of groups or clusters based on prior petrophysical or other geological data, is another way to improve these results (Rapstine, 2015; Sun & Li, 2016a, 2016b). Nowadays, the application of Fuzzy clustering can be seen in all fields of science and technology, especially for complex structured data and in cases of ambiguous or overlapping class boundaries. Considering these properties, the large, complex and ambiguous data of geophysics can benefit from fuzzy clustering in geophysics. Detecting geophysical anomalies such as mineral deposits, hydrocarbon reservoirs, faults and fractures (Miller et al., 2009), incorporating petrophysical information and different types of geophysical data in the geophysical interpretation (Bennington et al., 2015; Liao et al., 2022), and geological mapping of rock types (Wang et al., 2021) are a few examples of using fuzzy clustering in geophysics. This fuzziness concept is also used in seismic inversion (Kieu & Kepic, 2020). Fuzzy clustering is a form of clustering that allows the data to belong to more than one cluster with different degrees of membership (Bezdek et al., 1984). This creates more flexible and robust results than traditional clustering methods, such as k-means, which assign each data point to a single cluster (Bora & Gupta, 2014). Fuzzy clustering can account for the overlapping of acoustic impedance of different layers and features, which causes ambiguity in the interpretation of the models.

Fuzzy seismic inversion is a technique that uses fuzzy logic and fuzzy sets to estimate the uncertainty of seismic inversion results. Fuzzy logic is a form of multivalued logic that deals with reasoning that is approximate rather than fixed and exact. Fuzzy sets are sets whose elements have degrees of membership, rather than belonging or not belonging to the set. Fuzzy seismic inversion can provide more realistic and reliable information for seismic interpretation and reservoir characterization (Jahanjooy et al., 2023).

Structural, stratigraphic and petrophysical features of the subsurface can be revealed through measurements derived from seismic data known as seismic attributes (Bhatt & Helle, 2002). Different methods of calculation, extraction and interpretation of amplitude, frequency, phase and waveform attributes, create various types of seismic attributes (Chopra & Marfurt, 2005). These attributes can help to identify and characterize potential reservoirs, such as fluvial channel sands, carbonate reefs, or fractured zones (Oumarou et al., 2021). Channels can be challenging to image and delineate using conventional seismic amplitude data, due to their complex geometry, heterogeneity and lateral variability (Chopra & Marfurt, 2005). Therefore, seismic attribute analysis can be applied to enhance the visualization and understanding of fluvial channel features and processes.

In this paper, we present a case study of fuzzy seismic inversion applied to channel features in Johnson Formation of Browse Basin, Australia. The Browse Basin is a sedimentary basin located offshore of Western Australia, which contains several hydrocarbon discoveries. The Johnson Formation is a Late Jurassic to Early Cretaceous unit that consists of fluvial and marine sandstones, siltstones, and shales (Geoscience, 2023). We use the Poseidon seismic data, which covers an area of about 3000 km^2 in the Browse Basin, and well log data from the Poseidon-1 well. We use a seismic inversion objective function that uses multi-constraint terms including fuzzy clustering on different properties of the inversion results to create an acoustic impedance model of the Johnson Formation. The results reveal detailed subsurface channels. We compare this model to model-based seismic inversion results, seismic time slice and seismic attributes to show the efficiency of the multi-constrained fuzzy seismic inversion in creating geophysical models.

The structure and organization of this paper are as follows: Section 2 describes the study area and 3D seismic data of the Poseidon gas field. Section 3 reviews the theory and methodology of the model-based seismic inversion, fuzzy seismic inversion, and the seismic attributes that were applied to the seismic data. Section 4 qualitatively describes a channeled zone in the area of interest using the methods of section 2 and RGB blending of their results. Section 5 summarizes the main conclusions and implications of this paper.

2. Study Area and Data

The Browse Basin is a large sedimentary basin located offshore of Western Australia (Figure 1). The basin has a complex tectonic and stratigraphic evolution, involving six phases of deformation from the late Carboniferous to the late Miocene, with intermediate periods of Permian and Triassic thermal subsidence (Radlinski et al., 2004). The basin is a proven hydrocarbon province (Farfour et al., 2021), with major undeveloped gas and condensate fields in the outer and central basin and minor oil discoveries on the basin's eastern margin.

Several structural elements are detected in the Browse Basin, including the Leveque Shelf, Yampi Shelf, Barcoo Sub-basin, Caswell Sub-basin, Scott Plateau and Seringapatam Sub-basin. The main depocentres are the Caswell and Barcoo Sub-basins, which contain up to 15 km of sedimentary section and lie in a 100 to 1500 m water depth. The outer Browse Basin underlies the deep-water Scott Plateau (Rollet et al., 2016).

The stratigraphy of the Browse Basin is characterized by a major progradational clastic-to-carbonate cycle from the Carboniferous to the Tertiary (Figure 2). The Carboniferous section is predominantly fluvio-deltaic and the Permian-Early Triassic section is marine. Middle-Late Triassic rocks include fluvial and shallow marine clastics and minor carbonates. Early-Middle Jurassic syn-rift sediments comprise deltaic and coastal-plain clastics and coal. Widespread erosion occurred in the Callovian and Upper Jurassic sandstones and shales onlap, drape, and provide a thin regional seal across most pre-Callovian structures (Geoscience, 2023). Widespread transgression commenced in the Valanginian and peaked in the Turonian and resulted in the deposition of thick open marine claystone. The Turonian-Tertiary section records a major progradational clastic-to-carbonate cycle.

The Browse basin is classified into several formations (Figure 1). Some interpretations of Johnson and Wollaston formations indicate that they are deposited in a shallow marine environment. The paleotopography reconstruction revealed that the depositional environment was controlled by the structural highs and lows of the basin. Based on the seismic attributes, there are potential reservoir zones within the Johnson and Wollaston formations (Maulana, 2021).

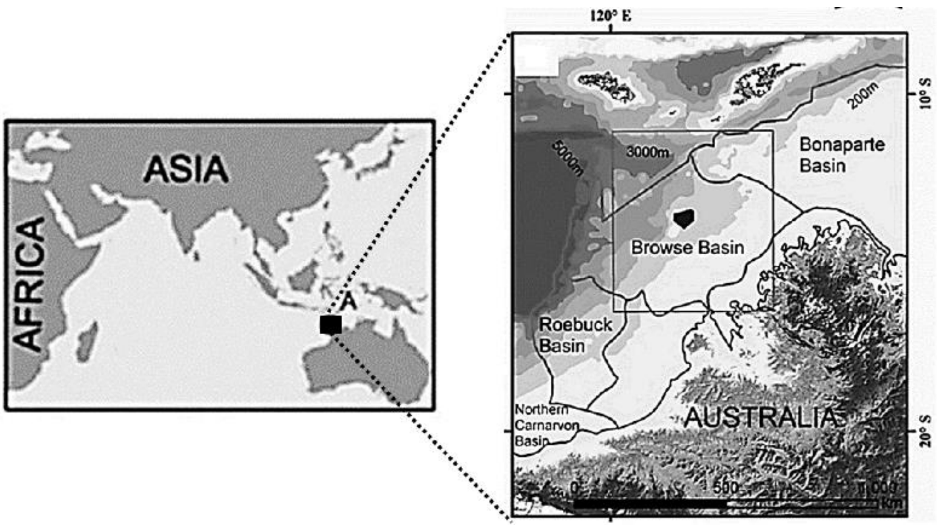

Figure 1. Location of the Browse Basin and the 3D Poseidon seismic data.

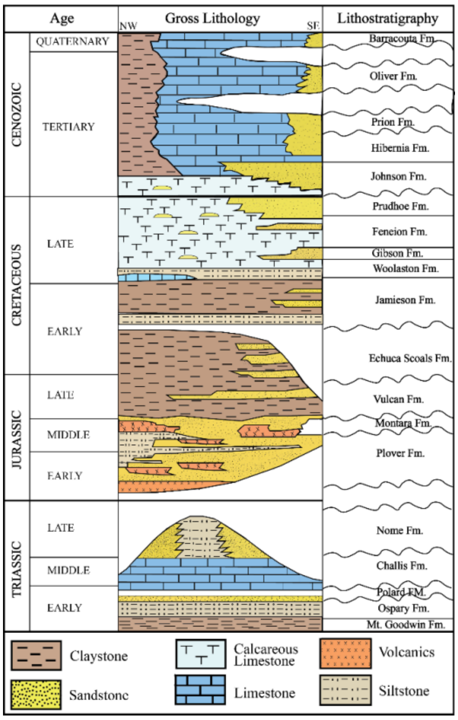

Figure 2. Litho-stratigraphic framework of Browse basin (Geoscience, 2023).

The Poseidon seismic data covers an area of about 3000 km^2 in the central part of the Browse Basin, overlying the Caswell Sub-basin and part of the Scott Plateau (Figure 4). The data was acquired in 2009 by Geoscience Australia and reprocessed in 2017 by ConocoPhillips using the pre-stack depth migration (PSDM) technique. The data has a bin size of 12.5 × 18.75 m and a sample interval of 4 ms (TerraNubis, 2023). A cropped version of this data is used in the inversion process. Both of the selected inline and crossline ranges are 1000–3000 in which the traces are selected in 5-trace intervals. The selected bin sizes are 95 m × 50 m (inline × crossline), while the sampling interval is 4 ms. The online density and sonic logs for the available wells are limited to a narrow depth. These logs are used to create an initial impedance model.

3. Theory

3-1. Model-Based Seismic inversion

In the post-stack seismic inversion, the goal is to create an acoustic impedance model whose synthetic seismic traces have a minimum misfit to the original seismic data:

$$\boldsymbol{\Phi}_d = \|\boldsymbol{d} - \mathbf{W}\boldsymbol{r}\|_2^2. \tag{1}$$

where d is the seismic traces, **W** is the convolution matrix of the wavelet, **r** is the reflectivity of the created model. For a continuous earth model, the reflectivity is related to the acoustic impedance of the j^{th} layer as $\boldsymbol{r}_j = (\boldsymbol{x}_{j+1} - \boldsymbol{x}_j)/2$ (Berteussen & Ursin, 1983). $\boldsymbol{x}_j$ is the natural logarithm of acoustic impedance of the j^{th} layer. In a recursive form, the above is rewritten as the following form:

$$\boldsymbol{x}_{j+1} - \boldsymbol{x}_j = 2\sum_{i=1}^{j} \boldsymbol{r}_i. \quad \boldsymbol{r} = [r_1. r_2. \dots . r_N]^T. \quad \text{(a)}$$

$$\boldsymbol{x} = \boldsymbol{H}\boldsymbol{r}, \quad \text{(b)}$$

$$\boldsymbol{H} = \begin{bmatrix} 0 & 0 & \cdots & 0 \\ 2 & 0 & \cdots & 0 \\ 2 & 2 & \cdots & 0 \\ \vdots & \vdots & \ddots & \vdots \\ 2 & 2 & \cdots & 2 \end{bmatrix}, \quad \text{(c)}$$

(2)

Additional constraints to the final model could prevent overfitting, reduce the effects of noise, add low-frequency information, and increase the uniqueness of this ill-posed inversion problem. For example, if the low-frequency trend of the model ($\boldsymbol{x}^{(0)}$) is obtainable from the well-logs and seismic horizons, adding a model term to the data misfit term ensures that the calculated model follows the general trend of the model:

$$\boldsymbol{\Phi}_x = \left\|\boldsymbol{x}^{(0)} - \mathbf{Hr}\right\|_2^2. \tag{3}$$

To ensure other properties in the result model, other terms such as smoothness ($\boldsymbol{\Phi}_s$) of the model (Jahanjooy et al., 2022), and sparsity ($\boldsymbol{\Phi}_r$) of the reflectivity are commonly used (Zhang & Castagna, 2011):

$$\boldsymbol{\Phi}_s = \|\boldsymbol{Dx}\|_2^2 = \|\boldsymbol{DHr}\|_2^2, \quad \text{(a)}$$
$$\boldsymbol{\Phi}_r = |\boldsymbol{r}|, \quad \text{(b)} \tag{4}$$

The D in the smoothness term referred to the vertical or horizontal difference matrix or a combination of them.

3-2. Fuzzy Seismic Inversion

The petrophysical data can be grouped into a few clusters that correspond to different geological settings in the subsurface. However, most of the seismic inversion methods do not account for the petrophysical data from well-logs and geological surveys. Adding a clustering term such as fuzzy clustering can introduce the initial petrophysical data to the inversion process and limit the inversion model to some known or unknown clusters. Well-logs, seismic interpretation, and/or geological settings are the sources for the known clusters:

$$\boldsymbol{\Phi}_{c\,(FCM)} = \sum_{j=1}^{M}\sum_{k=1}^{C}\boldsymbol{u}_{jk}^{q}\left\|\boldsymbol{x}_j - \boldsymbol{o}_k\right\|_2^2. \tag{5}$$

where $\boldsymbol{o}_k$ are the centroids of the clusters, while $\boldsymbol{u}_{jk}$ determines the membership of the j^{th} data sample to the k^{th} centroids (Bezdek et al., 1984).

The data misfit term ($\boldsymbol{\Phi}_d$) in Equation (1) has non-unique answers. Adding the model perturbation term ($\boldsymbol{\Phi}_x$) and a regularization term ensures a solution close to the initial low-frequency model. However, to consider various properties of the resulting model, Jahanjooy et al. (2023) have added a sparsity constraint on the reflectivity ($\boldsymbol{\Phi}_r = |\boldsymbol{r}|$) as well as a smoothness constraint ($\boldsymbol{\Phi}_s$) on the resulting model. Based on the spatial-temporal properties of the resulting model, smoothness could have several definitions. The clustering term added to the other mentioned constraints creates a multi-term objective function:

$$r = argmin_r\{\boldsymbol{\Phi}\} = argmin_r\{\alpha_d\boldsymbol{\Phi}_d + \alpha_x\boldsymbol{\Phi}_x + \alpha_s\boldsymbol{\Phi}_s + \alpha_c\boldsymbol{\Phi}_c + \boldsymbol{\Phi}_r\}. \tag{6}$$

The regularization parameters ($\alpha_.$) control the contribution of each term in the inversion process. Through a recursive process, the AI model of the j^{th} layer ($\boldsymbol{z}_j$) can be calculated ($\boldsymbol{z}_j = \boldsymbol{z}_1 e^{2\sum_{i=1}^{J} r_j}$). Figure 3 presents a flowchart for fuzzy seismic inversion using Equation (6). Well-tied post-stack seismic data and its interpreted horizons along with impedance logs can create an initial low-frequency model of the subsurface. If available, all the well-data and geological information can be clustered to an optimum number of clusters using a clustering method such as Fuzzy C-Means, FCM. The cluster number and centroids (if available) along with the seismic traces are used in the seismic inversion process. Considering the clustering term in the inversion process, this method also creates membership sections (or cubes) and cluster centers. The membership sections are sections that show the involvement of each point in each cluster center. The final cluster centers could differ from the initial cluster centers. This is due to the spatial variation of the model.

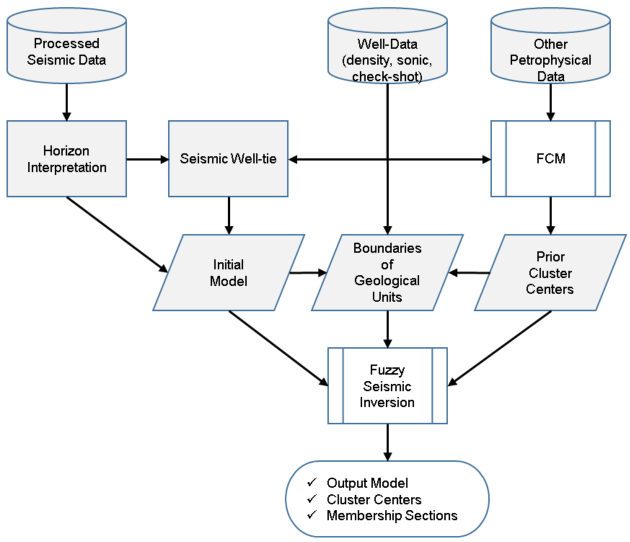

Figure 3. Flowchart of the fuzzy seismic inversion method.

3-3. Seismic Attributes

Numerous seismic attributes reveal and improve information in the seismic data based on time, amplitude, frequency, attenuation or other characteristics of seismic waves (Chopra & Marfurt, 2005). Among the various types of seismic attributes, geometric attributes are those that describe the shape and orientation of seismic features, such as faults, fractures, channels and salt bodies.

3D edge enhancement is a seismic geometric attribute that aims to improve the edge detection of seismic features by emphasizing larger and planar features in three dimensions. It is based on rotating a plane in all angles and directions and measuring the amplitude contrast along the plane. 3D edge enhancement can be used to detect structural or stratigraphic discontinuities, such as faults, fractures, channels or karst features (Mousavi et al., 2022). It can also be used as a fracture indicator or a noise reduction tool (Olaleye et al., 2021). Similarly, the convolve attributes are filters to smooth data and enhance the edges and contrasts (Liner, 2016). The event attribute measures the local peak or trough amplitude within a window and can highlight dominant reflections or diffractions. The RMS amplitude attribute measures the root mean square of the seismic amplitude values within a window and can reveal changes in lithology, porosity or fluid content. The semblance attribute measures the ratio of stacked energy to total energy within a window and can emphasize continuous or parallel reflections. The similarity attribute measures the degree of correlation between adjacent seismic traces and can enhance fault or channel boundaries. The texture attribute measures the spatial distribution of the seismic amplitude values within a window and can reveal subtle changes in lithology or porosity. The variance attribute is a seismic attribute that measures the standard deviation of the seismic amplitude values within a window. It can enhance fault or channel boundaries by showing high variance values along the discontinuities of the seismic waveforms (Chopra & Marfurt, 2007).

Acoustic impedance and seismic attributes both mirror the physical properties that influence the propagation and reflection of seismic waves. The correlation between these two sets of data makes them valuable in integrated applications for seismic inversion (Alabi & Enikanselu, 2019; Mardani & Thrust). Cumulative results of the inversion models and seismic attributes unveil vital details in hydrocarbon reservoirs characterization (Farfour et al., 2021; Zahmatkesh et al., 2018).

4. Results and Discussion

A cropped volume of the processed and stacked 3D Poseidon seismic data is used in the inversion process. The fuzzy seismic inversion is a time-consuming process that requires a high processing unit. To run the inversion on a personal computer with 12 gigabytes of ram and a 2.3 gigahertz processor, 80 percent of the traces are regularly omitted. Knowing that the fuzzy seismic inversion is a multidimensional process, the loss of input data affects the spatial resolution of the resulting model. Figure 4 shows the selected portion of the used 3D seismic data. Both of the used inlines and crosslines numbers 1000 to 3000 in which inline intervals are 75 m and crossline intervals are 50 m. The displayed time interval is from 2500 ms to 3000 ms.

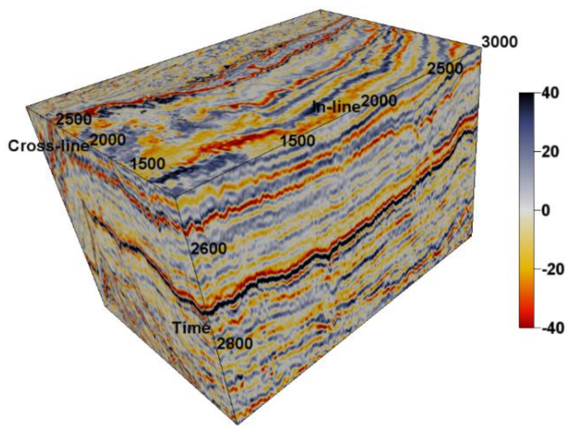

Figure 4. The selected cube of the used Poseidon 3D seismic data. Both the inlines and crosslines are from 1000 to 3000.

As an example, in the Johnson formation in the Poseidon field, Figure 5a shows a 2752 ms time slice of the seismic data. The arrows indicate a high amplitude curve. This event has been interpreted as the slopes of a submarine canyon on top of the Wollaston Formation (Liu, 2018). The width of the canyon can extend to several kilometers (Figure 5b). The upper part of the canyon is filled with channel-like features. These features are visible on the seismic 2752 ms time slice of Figure 5. The ellipse shape in Figure 5a encloses the area of interest. Due to the small dimension of such channel-like features, which are a few time samples along a few seismic traces, direct interpretation of them is challenging.

Two acoustic impedance models are created using model-based inversion and fuzzy model-based inversion (Figure 6a and b). The result of the model-based inversion is smoother, while the fuzzy model-based inversion has more contrast within layers and shows more detailed layering. Figure 7 displays the histogram of the time slice 2752 ms AI results. The model-based inversion result has created a normally distributed model, which could be nonrealistic in complex structures. The fuzzy seismic inversion result does not have a normal distribution. Although the fuzzy seismic inversion result has a skewness toward smaller AI, it covers a wider range and creates larger AI samples.

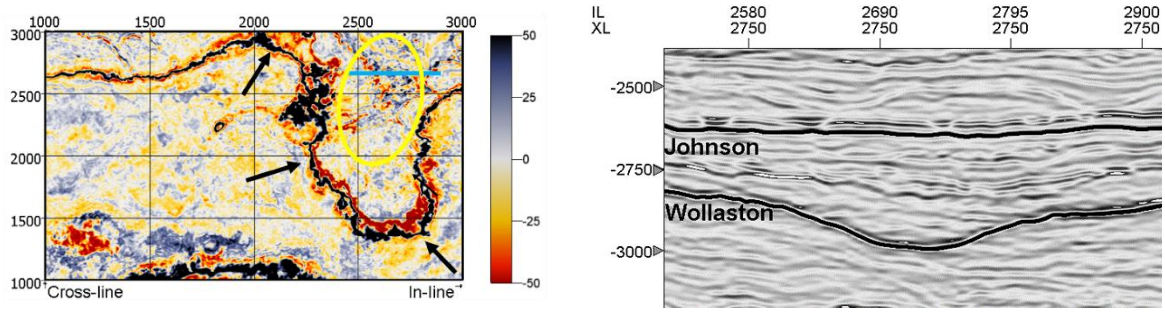

(a) (b)

Figure 5. (a) Seismic time slice at 2752ms. (b) Crossline 2750 of the seismic cube and two interpreted horizons. The blue line in a is the location of b in the study area.

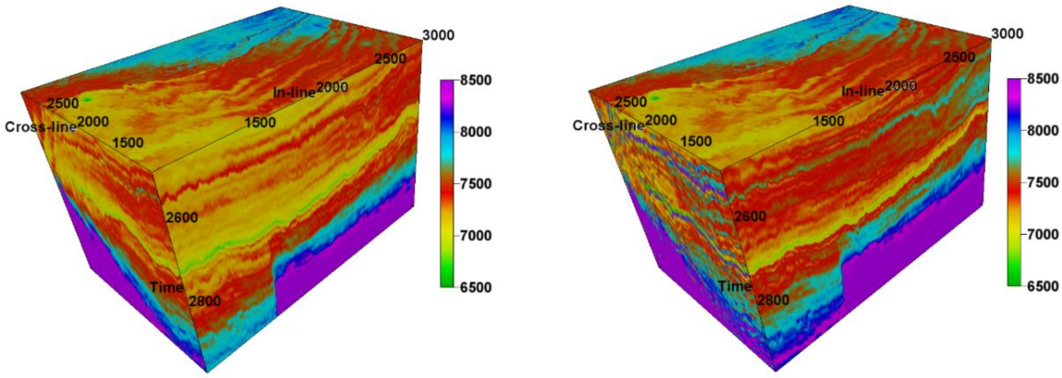

(a) (b)

Figure 6. The inversion result of the seismic cube of Figure 4 using model-based inversion (a) and fuzzy model-based inversion (b).

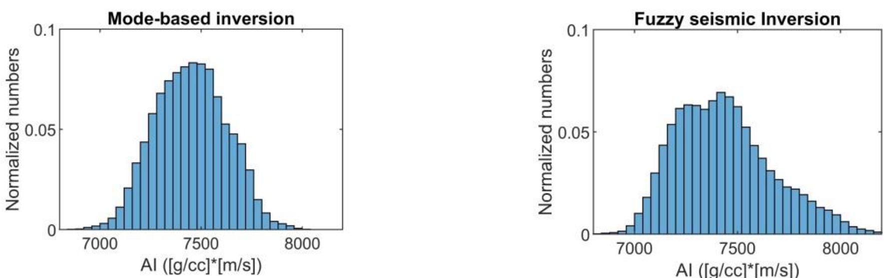

(a) (b)

Figure 7. Histogram of the AI model at time slice 2752 ms for model-based inversion (a) and fuzzy inversion (b).

The channeled zone is visible in the acoustic impedance time slices (Figure 8a and b). In the AI result of the model-based inversion, the geometry of the channeled zone follows the amplitudes in the seismic data (Figure 8a). However, the direction of the higher acoustic impedance zone of these features is slightly different in the fuzzy inversion method. An additional output of the fuzzy inversion is the high-resolution reflectivity data. The interest features have created a reflectivity anomaly in the study zone (Figure 8c).

Some wells in the Poseidon field are used to create the initial model. However, there is not any well-data in the area of interest. Therefore, to check the AI results for the channeled zone, this study performs a qualitative examination of the morphology and direction of the channeled zone using seismic attributes. Among numerous seismic attributes that can be helpful to define the geometry of subsurface channels, those which have created anomalies in the study data are 3DEE, convolution, event, RMS amplitude, semblance, similarity, texture and variance.

Seismic attributes at the 2752 ms time slice are displayed in Figure 9. In addition to the canyon's edge, the subtle channel features are appearing in the time slice of the 3DEE. Compared to the seismic time slice, there is an enhanced convolve values along the channel, indicating the amplification of the seismic signal. In the event attribute, there are relatively strong event values along the channel, indicating the presence of significant seismic events. Although the slopes of the submarine canyon create a high RMS amplitude attribute, there are some high-energy seismic reflections in the area of interest. The coherence of the seismic events along the channeled zone is evident in the semblance attribute. Values with low similarity along the channel edges indicate the discontinuities of the seismic waveforms. In the texture attribute, there are variations of the local seismic texture along the channel axis and across the channel width. The channeled zone is also manifested as small meandering features in the variance attribute.

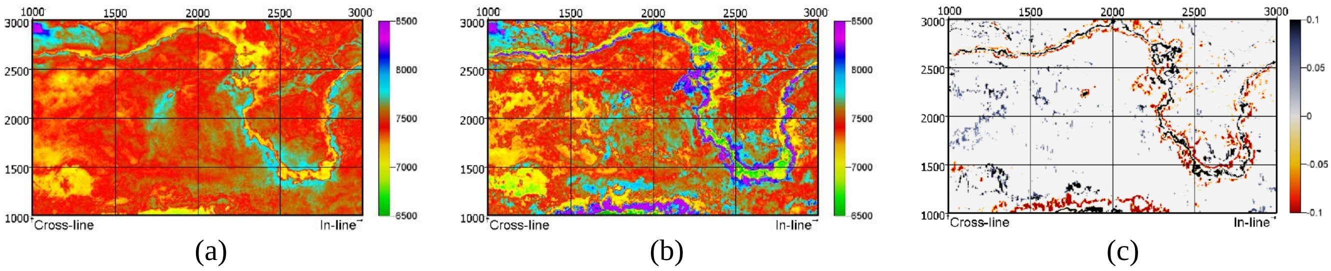

Figure 8. The result time slices at 2752 ms. (a) AI model obtained using model-based inversion. (c) AI model obtained using fuzzy seismic inversion (c) reflectivity time slice.

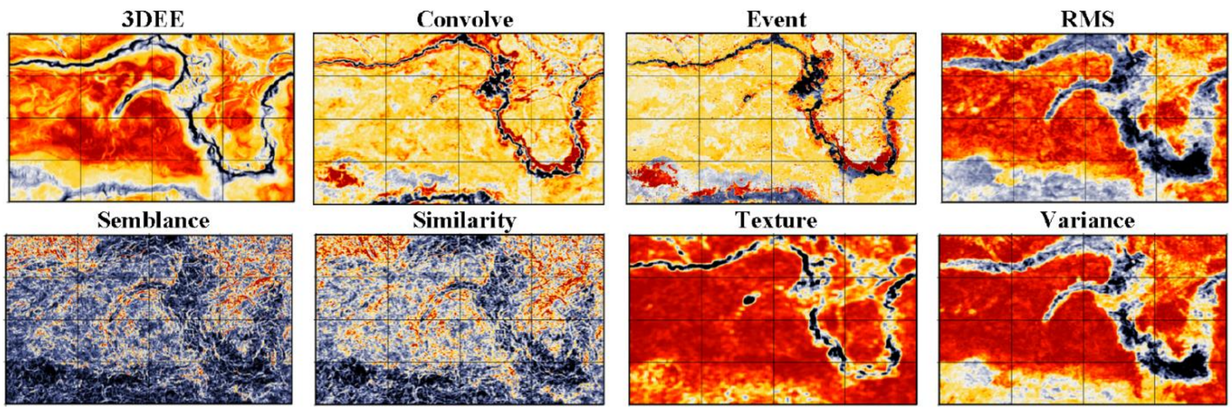

Figure 9. Seismic attribute result on time-slice 2750 ms. All of these attributes are consistent with the AI result and show anomalies in the area of interest.

Aside from the AI model and the reflectivity cube genuine outputs of the fuzzy model-based inversion of the 3D seismic data are the 3D membership cubes. Each element of the cube defines the membership of a time sample to one of the classes, from zero to one. The optimum number of classes is usually selected by using the elbow method (Krzanowski & Lai, 1988) on well-log data or geological information. In our case, there was not enough well-data in the inversion zone. Using geological information, this number is selected as 4, which is consistent with the information on the inversion zone in Figure 2. Membership data for the time-slice 2752 ms is displayed in Figure 10. The order and naming of the classes are arbitrary. Knowing that this data is created by the classification of the impedances, their values follow the impedance changes rather than geological features and seismic facies. However, some general pattern appears in the membership section, which can be helpful along with other data.

In the seismic interpretation, the RGB blending technique that combines two or more seismic attributes into a single color image using the red-green-blue (RGB) color model enables the interpreter to visualize multiple aspects of the seismic data simultaneously and to highlight subtle features that may not be evident in a single attribute display. In Figure 10, memberships to cluster 1 is approximately zero in the area of interest and one elsewhere. This membership time slice along with the seismic data and the impedance result of the fuzzy model-based inversion is used in an RGB blending. The result in Figure 11a shows the highlighting of the channels in the RGB image. The RGB blending is repeated using the 3DEE attribute instead of the impedance time slice. The result in Figure 11b is relatively similar to the previous case. However, as can be expected, the 3DEE attribute enabled a finer detection of larger structures such as the canyon. Although it is not displayed here, the results of using the other attributes instead of the 3DEE in this RGB are similar.

The values of cluster 2 in the area of interest are nearly one. Some subtle variations in this cluster are visible in the area of interest. 'The process in Figure 11a was repeated using cluster 2 and the results are displayed in Figure 11c. Although the channel zone is not clear in this RGB image, using cluster 2 creates a more detailed image in other zones of the time slice.

The memberships (Figure 10) can be considered as attributes that determine the degree of belonging of the data samples to each impedance cluster. Figure 11d shows the RGB blending result of clusters 1, 2 and 3. The channels cannot be identified directly in this image. However, due to the intrinsic purpose and content of the membership clusters and given that the general slope of the Johnson formation is S-N, the main depositional environments in the formation are distinguishable.

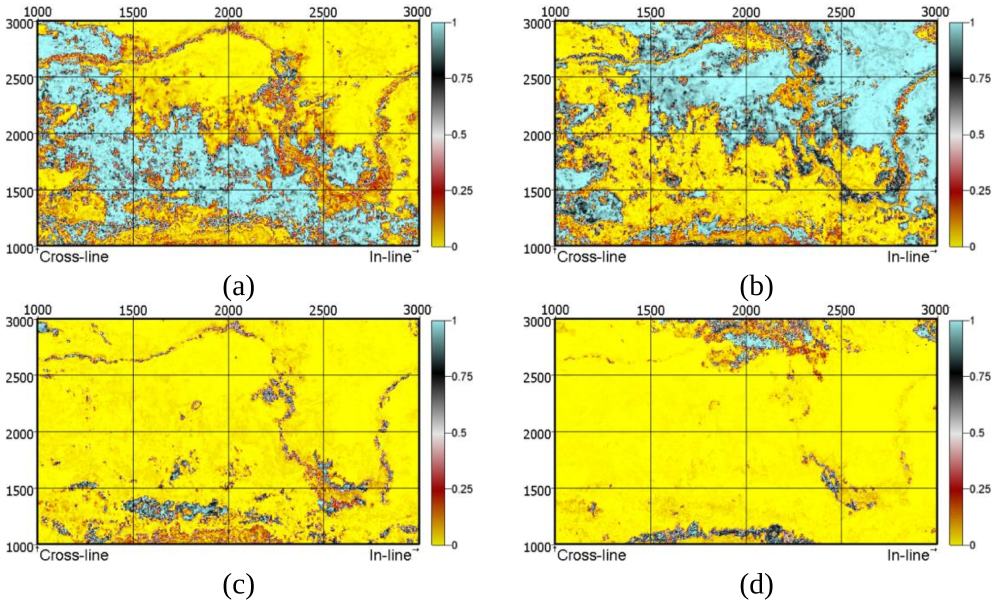

Figure 10. Membership time slice of 2620ms. (a) Cluster 1. (b) Cluster 2. (c) Cluster 3. (d) Cluster 4.

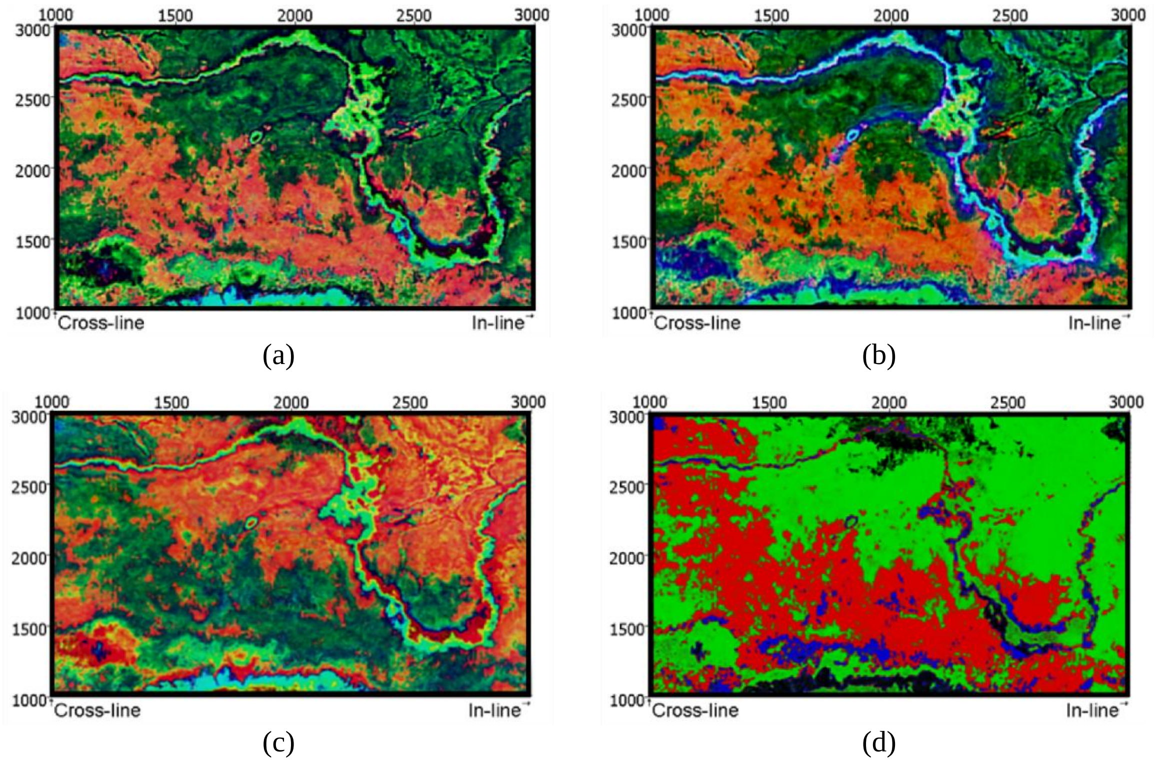

Figure 11. RGB blending results of 2752 ms time slice. (a) RGB of cluster 1, seismic data, and the acoustic impedance of fuzzy model-based inversion. (b) RGB of cluster 1, seismic data, and 3DEE attribute. (c) RGB of cluster 2, seismic data, and the acoustic impedance of fuzzy model-based inversion. (d) RGB of cluster 1, cluster 2, cluster 3.

5. Conclusions

This paper uses a multi-constrain multi-dimension fuzzy model-based seismic inversion method based on prior information and fuzzy clustering constraints to create more realistic and robust acoustic impedance models. The method can handle the non-uniqueness, ambiguity, and noise of the seismic inversion problem by incorporating multiple terms in the objective function, such as data misfit, model perturbation, sparsity, smoothness and clustering. This inversion method is applied to a cropped cube of the 3D Poseidon seismic data from the Browse Basin, offshore Western Australia, comparing the results with conventional model-based inversion. The fuzzy model-based inversion method has produced higher resolution, contrast, and stability in the acoustic impedance models and revealed more details of the subsurface structures. Qualitative comparison and cooperation of the inversion result and seismic attributes are performed. The result of fuzzy seismic inversion is consistent with the seismic attributes. Membership cubes are the additional outputs of the fuzzy inversion process. To enhance the interpretation of the seismic features, such as submarine channels, canyons, and depositional environments, memberships are used along with the seismic data and seismic attributes in the RGB blending. The result has shown good agreement with the acoustic impedance models and highlighted subtle features that may not be evident in a single attribute display. The proposed method and attributes can be useful tools for seismic data interpretation and reservoir characterization in complex geological settings. There are several researches and reports on the Poseidon gas field. By prestack interpretation and drilling exploration wells in the area of interest, we could improve our understanding of the reservoir potential of the studied channeled zone.

References

Alabi, A., & Enikanselu, P. A. (2019). Integrating seismic acoustic impedance inversion and attributes for reservoir analysis over ‘DJ’Field, Niger Delta. *Journal of Petroleum Exploration and Production Technology*, 9, 2487-2496.

Bennington, N. L., Zhang, H., Thurber, C. H., & Bedrosian, P. A. (2015). Joint inversion of seismic and magnetotelluric data in the Parkfield Region of California using the normalized cross-gradient constraint. *Pure and Applied Geophysics*, 172(5), 1033-1052.

Berteussen, K., & Ursin, B. (1983). Approximate computation of the acoustic impedance from seismic data. *Geophysics*, 48(10), 1351-1358.

Bezdek, J. C., Ehrlich, R., & Full, W. (1984). FCM: The fuzzy c-means clustering algorithm. *Computers & Geosciences*, 10(2-3), 191-203.

Bhatt, A., & Helle, H. B. (2002). Determination of facies from well logs using modular neural networks. *Petroleum Geoscience*, 8(3), 217-228.

Bosch, M., Mukerji, T., & Gonzalez, E. F. (2010). Seismic inversion for reservoir properties combining statistical rock physics and geostatistics: A review. *Geophysics*, 75(5), 75A165-175A176.

Chopra, S., & Marfurt, K. J. (2005). Seismic attributes—A historical perspective. *Geophysics*, 70(5), 3SO-28SO.

Chopra, S., & Marfurt, K. J. (2007). *Seismic attributes for prospect identification and reservoir characterization*. Society of Exploration Geophysicists and European Association of of Geoscientists and Engineers.

Das, V., & Mukerji, T. (2020). Petrophysical properties prediction from prestack seismic data using convolutional neural networks. *Geophysics*, 85(5), N41-N55.

Farfour, M., El-Ghali, M. A., Gaci, S., Moustafa, M. S., & Siddiqui, N. A. (2021). Seismic attributes for hydrocarbon detection and reservoir characterization: a case study from Poseidon field, Northwestern Australia. *Arabian Journal of Geosciences*, 14, 1-11.

Geoscience, A. (2023). *Regional Geology of the Browse Basin*. https://www.ga.gov.au/scientific-topics/energy/province-sedimentary-basin-geology/petroleum/acreagerelease/browse

Jahanjooy, S., Hashemi, H., & Bagheri, M. (2023). *Multi-dimensional, Multi-Constraint, Deconvolution, Denoising, and Seismic Inversion Using Hard and Fuzzy Clustering Concepts [Manuscript submitted for publication]*.

Jahanjooy, S., Riahi, M. A., & Moghanloo, H. G. (2022). Blind inversion of multidimensional seismic data using sequential Tikhonov and total variation regularizationsBlind seismic inversion using STTVR. *Geophysics*, 87(1), R53-R61.

Kieu, D. T., & Kepic, A. (2020). Seismic-impedance inversion with fuzzy clustering constraints: An example from the Carlin Gold district, Nevada, USA. *Geophysical Prospecting*, 68(1-Cost-Effective and Innovative Mineral Exploration Solutions), 103-128.

Krzanowski, W. J., & Lai, Y. (1988). A criterion for determining the number of groups in a data set using sum-of-squares clustering. *Biometrics*, 23-34.

Liao, C., Hu, X., Zhang, S., Li, X., Yin, Q., Zhang, Z., & Zhang, L. (2022). Joint inversion of gravity, magnetotelluric and seismic data using the alternating direction method of multipliers. *Geophysical Journal International*, 229(1), 203-218.

Liner, C. L. (2016). *Elements of 3D seismology*. Society of exploration geophysicists.

Liu, Z. (2018). *Seismic geomorphology of continental margin evolution in the late Cretaceous to Neogene of the Browse Basin, northwest Australia*. Colorado School of Mines.

Mardani, R. A., & Thrust, G. V. Estimation of Acoustic Impedance from Seismic Data in Well-log Resolution Using Machine Learning, Neural Network, and Comparison with Band-limited Seismic Inversion.

Maulana, I. D. P. A. D. M. C. J. M. I. R. F. (2021). *Analyzing Shallow Marine Depositional Environment using Paleotopography Reconstruction and RGB Blending - Case Study: Woolaston and Johnson Formation, Poseidon Field, Browse Basin* Joint Convention Bandung, Bandung.

Miller, D. J., Nelson, C. A., Cannon, M. B., & Cannon, K. P. (2009). Comparison of fuzzy clustering methods and their applications to geophysics data. *Applied Computational Intelligence and Soft Computing*, 2009, 1-9.

Mousavi, J., Radad, M., Soleimani Monfared, M., & Roshandel Kahoo, A. (2022). Fault enhancement in seismic images by introducing a novel strategy integrating attributes and image analysis techniques. *Pure and Applied Geophysics*, 179(5), 1645-1660.

Olaleye, O. K., Enikanselu, P. A., & Ayuk, M. A. (2021). Characterization of reservoir sands using 3D seismic attributes in the coastal swamp area of Niger Delta Basin. *Journal of Petroleum Exploration and Production Technology*, 11, 3995-4004.

Oumarou, S., Mabrouk, D., Tabod, T. C., Marcel, J., Ngos III, S., Essi, J. M. A., & Kamguia, J. (2021). Seismic attributes in reservoir characterization: an overview. *Arabian Journal of Geosciences*, 14, 1-15.

Pintea, S. L., Sharma, S., Vossepoel, F. C., van Gemert, J. C., Loog, M., & Verschuur, D. J. (2021). Seismic inversion with deep learning: A proposal for litho-type classification. *Computational Geosciences*, 1-14.

Radlinski, A., Kennard, J., Edwards, D., Hinde, A., & Davenport, R. (2004). Hydrocarbon generation and expulsion from Early Cretaceous source rocks in the Browse Basin, North West Shelf, Australia: a small angle neutron scattering study. *The APPEA Journal*, 44(1), 151-180.

Rapstine, T. D. (2015). *Gravity gradiometry and seismic interpretation integration using spatially guided fuzzy c-means clustering inversion*. Colorado School of Mines.

Rollet, N., Grosjean, E., Edwards, D., Palu, T., Abbott, S., Totterdell, J., Lech, M., Khider, K., Hall, L., & Orlov, C. (2016). New insights into the petroleum prospectivity of the Browse Basin: the results of a multi-disciplinary study. *The APPEA Journal*, 56(1), 483-494.

Rosa, D. R., Santos, J. M., Souza, R. M., Grana, D., Schiozer, D. J., Davolio, A., & Wang, Y. (2020). Comparing different approaches of time-lapse seismic inversion. *Journal of Geophysics and Engineering*, 17(6), 929-939.

Russell, B., & Hampson, D. (1991). Comparison of poststack seismic inversion methods. In *SEG Technical Program Expanded Abstracts 1991* (pp. 876-878). Society of Exploration Geophysicists.

Sun, J., & Li, Y. (2016a). Joint inversion of multiple geophysical and petrophysical data using generalized fuzzy clustering algorithms. *Geophysical Supplements to the Monthly Notices of the Royal Astronomical Society*, 208(2), 1201-1216.

Sun, J., & Li, Y. (2016b). Joint inversion of multiple geophysical data using guided fuzzy c-means clustering. *Geophysics*, 81(3), ID37-ID57.

TerraNubis (2023). *Project NW Shelf Australia - Poseidon 3D*. Retrieved July 28,2023 from https://terranubis.com/datainfo/NW-Shelf-Australia-Poseidon-3D

Wang, Y., Ksienzyk, A. K., Liu, M., & Brönner, M. (2021). Multigeophysical data integration using cluster analysis: assisting geological mapping in Trøndelag, Mid-Norway. *Geophysical Journal International*, 225(2), 1142-1157.

Zahmatkesh, I., Kadkhodaie, A., Soleimani, B., Golalzadeh, A., & Azarpour, M. (2018). Estimating Vsand and reservoir properties from seismic attributes and acoustic impedance inversion: A case study from the Mansuri oilfield, SW Iran. *Journal of Petroleum Science and Engineering*, 161, 259-274.

Zhang, R., & Castagna, J. (2011). Seismic sparse-layer reflectivity inversion using basis pursuit decomposition. *Geophysics*, 76(6), R147-R158.